ResearchGate

See discussions, stats, and author profiles for this publication at: https://www.researchgate.net/publication/230725172

Growth Mechanism of Single-Walled Carbon Nanotubes on Iron–Copper Catalyst and Chirality Studies by Electron Diffraction

ARTICLE *in* CHEMISTRY OF MATERIALS · APRIL 2012

Impact Factor: 8.35 · DOI: 10.1021/cm300308k

CITATIONS
21

READS
46

15 AUTHORS, INCLUDING:

Maoshuai He
Aalto University
34 PUBLICATIONS **820** CITATIONS
SEE PROFILE

Elena D Obraztsova
Russian Academy of Sciences
276 PUBLICATIONS **3,292** CITATIONS
SEE PROFILE

Ilya V. Anoshkin
Aalto University
65 PUBLICATIONS **470** CITATIONS
SEE PROFILE

Albert G Nasibulin
Skolkovo Institute of Science and Technology
234 PUBLICATIONS **3,849** CITATIONS
SEE PROFILE

Available from: Elena D Obraztsova
Retrieved on: 30 January 2016

CHEMISTRY OF MATERIALS

Article

pubs.acs.org/cm

Growth Mechanism of Single-Walled Carbon Nanotubes on Iron–Copper Catalyst and Chirality Studies by Electron Diffraction

Maoshuai He,*[,†] Bilu Liu,[‡,§] Alexander I. Chernov,[∥] Elena D. Obraztsova,[∥] Inkeri Kauppi,[†] Hua Jiang,[‡] Ilya Anoshkin,[‡] Filippo Cavalca,[⊥] Thomas W. Hansen,[⊥] Jakob B. Wagner,[⊥] Albert. G. Nasibulin,[‡] Esko I. Kauppinen,*[,‡] Juha Linnekoski,[†] Marita Niemelä,[†] and Juha Lehtonen[†]

[†]Department of Biotechnology and Chemical Technology, School of Chemical Technology, Aalto University, P.O. Box 16100, FI-00076 Aalto, Finland

[‡]NanoMaterials Group, Department of Applied Physics and Center for New Materials, School of Science, Aalto University, P.O. Box 15100, FI-00076 Aalto, Finland

[§]Shenyang National Laboratory for Materials Science, Institute of Metal Research, Chinese Academy of Sciences, Shenyang 110016, P. R. China

[∥]A. M. Prokhorov General Physics Institute RAS, 38 Vavilov Street, 119991 Moscow, Russia

[⊥]Center for Electron Nanoscopy, Technical University of Denmark, DK-2800 Kgs Lyngby, Denmark

Supporting Information

ABSTRACT: Chiralities of single-walled carbon nanotubes grown on an atomic layer deposition prepared bimetallic FeCu/MgO catalyst were evaluated quantitatively using nanobeam electron diffraction. The results reveal that the growth yields nearly 90% semiconducting tubes, 45% of which are of the (6,5) type. The growth mechanisms as well as the roles of different components in the catalyst were studied in situ using environmental transmission electron microscopy and infrared spectroscopy. On the basis of the understanding of carbon nanotube growth mechanisms, an MgO-supported FeCu catalyst was prepared by impregnation, showing similar catalytic performance as the atomic layer deposition-prepared catalyst, yielding single-walled carbon nanotubes with a similar narrow chirality distribution.

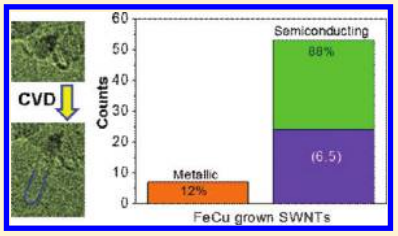

KEYWORDS: *single-walled carbon nanotube, semiconducting SWNTs, electron diffraction, iron–copper catalyst*

INTRODUCTION

Because of their unique and extraordinary properties, carbon nanotubes, especially single-walled carbon nanotubes (SWNTs), have been the subject of studies in a vast range of domains since their discovery.[1−3] The electronic and optical properties of SWNTs depend on their atomic structures, which are uniquely indexed with their chiral indices (n,m).[4] A pristine SWNT can be either metallic or semiconducting depending on whether mod $(n-m, 3) = 0$ or mod $(n-m, 3) = 1$ or 2. SWNTs with controlled chirality and conductivity are highly desirable for both fundamental research and practical applications.[5,6] Prototypes of conductors[7] made from metallic SWNT networks and field effect transistors[8] from semiconducting SWNTs have already been demonstrated, but their wide applications are limited because most of the as-produced SWNTs have a broad diameter range and contain a mixture of semiconducting and metallic species.[9,10]

In the past decade, significant progress has been made in the postsynthesis sorting of SWNTs according to their conductivity and chirality.[5,11−13] A number of methods like electrophoresis[13] and density gradient ultracentrifugation[11] have been developed. However, most of the postsynthesis sorting schemes are tedious and costly. Moreover, the solution-based processes inevitably introduce impurities onto tube walls resulting in a loss of their optimal device performance. Chemical vapor deposition (CVD) growth is considered as the most economic process to obtain SWNTs with preferential metallic,[14] semiconducting,[15,16] or particular (n,m) species.[17,18] A certain degree of control on SWNT structure has been achieved by varying growth parameters including carbon source,[19] catalyst composition,[20] and concentration of H_2O vapor[14] or NH_3,[21] among which the development of new catalyst systems is of utmost importance for selective growth of SWNTs. As verified by various spectroscopic methods,[9,22,23] catalytic systems like CoMo[9,22] and CoMn[23] can favor the growth of semiconducting SWNTs at low growth temperatures.

In our previous work,[24] we developed an MgO-supported FeCu catalyst for highly efficient growth of SWNTs in which both the support and the catalyst can be easily removed by mild acid treatment after growth. As evaluated by UV–vis-NIR absorption and photoluminescence (PL) spectra, predominant (6,5) tube growth was achieved for the product synthesized at 600 °C. However, PL is intrinsically blind to metallic SWNTs, and the peaks in the absorption spectrum cannot be

Received: January 27, 2012
Revised: April 11, 2012
Published: April 19, 2012

ACS Publications © 2012 American Chemical Society

individually resolved. More importantly, there are no reliable correlations between the intensity and the concentration in both techniques. Therefore, neither the fraction of semiconducting SWNTs nor the concentration of (6,5) tubes in the FeCu grown SWNTs has been accurately determined. Meanwhile, there are many other issues that need to be clarified in order to understand the growth mechanisms of catalyst nucleation and SWNT growth. For example, how do the Fe catalyst particles nucleate? What are the roles of MgO and CuO? Can SWNTs grow from catalysts supported by the metallic Cu? To deal with these issues, in situ characterization techniques would provide better insight into these questions.

In this work, we study the (n,m) distribution of SWNTs grown on the MgO-supported FeCu catalyst at 600 °C using electron diffraction (ED). A high fraction of (6,5) tubes in particular, as well as of semiconducting tubes in general, were found. In situ environmental transmission electron microscopy (ETEM) and infrared (IR) spectroscopy studies were carried out to gain insight into the catalyst nucleation and SWNT growth mechanisms. This fundamental understanding would guide the preparation of a FeCu catalyst by a more economic impregnation approach.

EXPERIMENTAL SECTION

Characterization of SWNTs by Electron Diffraction. The SWNTs used for ED characterizations were grown at ambient pressure on a FeCu/MgO catalyst prepared by atomic layer deposition. The growth details are reported in a previous study.[24] The as-grown sample was purified by 3 M HCl and dispersed in 2 wt % sodium cholate aqueous solution. The suspension was centrifuged (100 000g for 40 min) and only the supernatant was collected. It is noteworthy to mention that the centrifugation does not affect the SWNT diameter distribution or bias a certain helicity distribution. A few drops of acetone were added to the supernatant and a copper TEM grid coated with a lacey carbon film was used for collecting the precipitate. After washing with acetone, methanol and isopropanol, the collected SWNTs were annealed at 400 °C in vacuum ($<10^{-5}$ Pa) for 2 h. The samples were investigated using a JEOL-2200FS double aberration-corrected microscope operated at 80 kV. The (n,m) determination from electron diffraction patterns of individual SWNTs was based on a calibration-free intrinsic layer line-spacing method.[27]

In Situ ETEM Investigations on FeCu Catalyst Reduction and SWNT Growth. The in situ ETEM experiments were performed on an aberration corrected FEI Titan 80-300FEG ETEM operated at 300 kV. The FeCu/MgO catalyst powder was dispersed on a bare Au grid, which was then loaded in a specimen holder and later inserted into the TEM chamber for in situ experiments. CO at a flow rate of 2 sccm was introduced into the microscope chamber and kept at a pressure of 290 Pa. The reduction of CuO particles was monitored using electron energy loss spectroscopy (EELs), while the temperature was increased slowly to 400 °C. Small Fe particle formation and SWNT growth were investigated by bright field TEM and high-angle annular dark-field scanning transmission electron microscopy (STEM) from 600 to 690 °C with pressures ranging from 290 to 620 Pa (CO flow rate: 2 to 4 sccm).

Time-Resolved FT-IR Spectroscopy of CO Interaction with FeCu Catalyst. The interaction of CO with catalyst surface under reaction conditions was studied by in situ diffuse reflectance infrared Fourier transform spectroscopy (DRIFTS). The DRIFTS measurements were performed using a Nicolet Nexus FTIR spectrometer and a Spectra-Tech high temperature/high pressure reaction chamber with ZnSe windows. The spectrum of an aluminum mirror measured under nitrogen flow was used as the background. The total gas flow rate was kept at 50 sccm.

A fresh sample was heated under nitrogen flow until the reaction temperature (600 °C) was reached. At 600 °C, diluted CO (2 vol % CO in N_2) was introduced into the cell, and IR spectra were acquired every 45 s (4 cm^{-1}, 30 scans) for approximately 10 min. After the experiment, the reactor cell was flushed with nitrogen.

RESULTS AND DISCUSSIONS

Nanobeam Diffraction of FeCu/MgO-Grown SWNTs. Nanoarea ED[1,25−27] has been used to determine the structure of SWNTs since their discovery. In contrast to various spectroscopic methods, which can only detect SWNTs with optical response, ED does not have such a limitation and provides an accurate way of measuring SWNT chirality. Figure 1a shows a typical TEM image of both bundled and individual

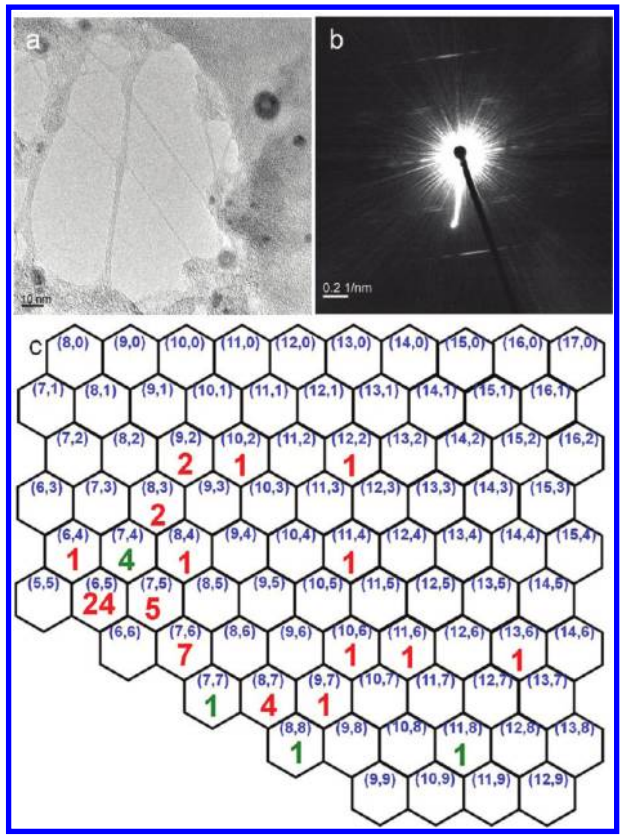

Figure 1. (a) Typical TEM image of well-dispersed SWNTs grown on FeCu/MgO catalyst with CO at 600 °C. (b) Nanobeam electron diffraction pattern from a (6,5) tube. (c) Chirality map of SWNTs grown on FeCu/MgO catalyst. The (n,m) populations were labeled with numbers in the hexagonal cell. Red numbers and green numbers correspond to semiconducting and metallic SWNTs, respectively.

SWNTs grown at 600 °C. An ED pattern of an isolated SWNT was shown in Figure 1b, which is featured by a set of parallel diffracted layer lines in addition to the bright spot at the center caused by the direct electron beam irradiation. The diffraction layer lines are separated by certain distances from the equatorial layer line at the center. By layer line distance analysis based on a novel concept of intrinsic layer line spacing,[27] the diffraction pattern has been indexed, and the chiral indices of the SWNT were determined to be (6,5). In agreement with optical characterization results, (6,5) tubes are found to be the most abundant species. ED patterns were recorded from 60 individual SWNTs, 24 of which were assigned to (6,5) tubes (40%, Figure 1c and Supporting Information, Table S1). In addition to (6,5) tubes, other near-armchair tubes, like (7,5), (7,6), and (8,7), are the major semiconducting species in the

dx.doi.org/10.1021/cm300308k | Chem. Mater. 2012, 24, 1796−1801

sample. The findings are in agreement with theoretical predictions that large-chiral-angle SWNTs are abundant in grown SWNTs.[28,29] This is because the cap preferred for forming a near-armchair SWNT is more stable than other caps. The (7,4) tubes, which exhibit a similar diameter as the (6,5) tubes, are the most abundant metallic species. The metallic fraction also consists of armchair tubes, such as (7,7) and (8,8) tubes. The diameter distribution deduced from the chiral indices (Supporting Information, Figure S1a) indicates that most of the tubes have diameters smaller than 1.0 nm. This diameter distribution is consistent with that measured from TEM images (Supporting Information, Figure S1b).

Compared with other SWNTs grown at high reaction temperatures,[10,21] the SWNTs grown on FeCu catalyst at 600 °C contain less helicity varieties. More important, the ED recording results show a semiconducting content of 88%, much higher than the typical semiconducting distribution. Different from other selective semiconducting SWNT growth, such as plasma[15] or ultraviolet[16] CVD, which preferentially destroy metallic SWNTs, this methodology produces SWNTs without degrading their properties. In addition, out of 60 investigated SWNTs, 51 (85%) have a chiral angle larger than 20°. All the results indicate that low temperature growth provides a robust means to control the atomic structure of SWNTs.

Investigations of SWNT Growth Mechanism. ETEM and EELS were used to monitor the nucleation of the catalytic Fe particles, the evolution of the CuO phase as well as the growth of SWNTs. Figure 2a,b shows TEM and STEM images of the prepared FeCu/MgO catalyst, respectively. Nanoparticles of size above 50 nm in diameter are seen on the MgO surface. These particles are identified as CuO with EELS, while hardly any isolated Fe particles are visible. These observations are in agreement with previous XRD characterizations,[24] where only the peaks corresponding to CuO and

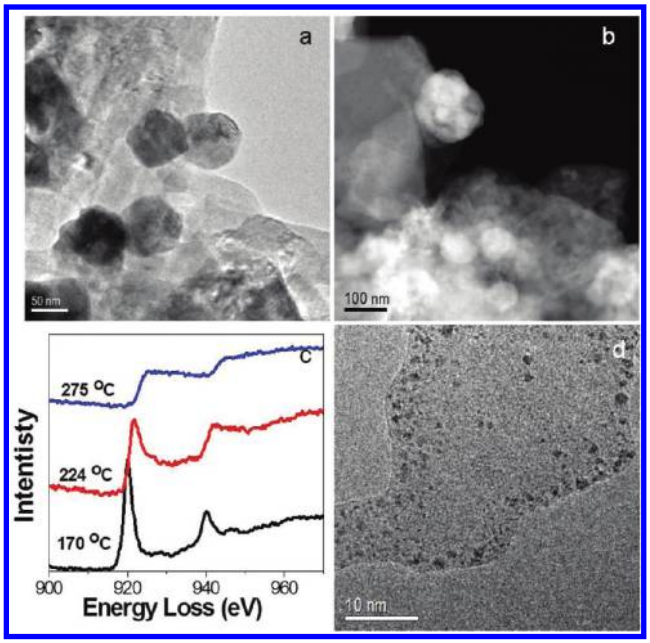

Figure 2. (a) Bright field TEM image and (b) high-angle annular dark-field STEM image of FeCu/MgO catalyst. (c) Evolution of the electron energy-loss spectra of Cu phase during reduction in CO atmosphere (290 Pa) at different temperatures. (d) TEM image showing the formation of small particles on MgO at 600 °C with a CO pressure of 290 Pa.

MgO were observed. The FeO phase is not observed as it forms a complete solid solution with MgO.[30] It is remarked that the possibility of forming a solid solution of CuO and MgO cannot be ruled out as they also have the same halite NaCl structure.[31]

The reducibility of CuO particles was studied by CO reduction at ~290 Pa in the TEM chamber. The characteristic $L_{2,3}$ edges of CuO (Figure 2c) in the EEL spectrum shows that no reduction occurred at temperatures below 180 °C, while partial reduction of Cu^{2+} ions to Cu^{+} or Cu^{0} took place in the temperature range from 180 to 275 °C. Finally, complete reduction of CuO to metallic Cu was observed at temperatures above 275 °C. Characteristic $L_{2,3}$ edges of Fe were also observed in the EEL spectrum on Cu particle surfaces (Supporting Information, Figure S2). As metallic Cu and Fe are immiscible, Fe can only exist on the surface of the reduced Cu in the form of small particles. This is quite reasonable considering the sequence for depositing Cu- and Fe-containing precursors on MgO support during the catalyst preparation process.[24]

When the temperature exceeded 600 °C, the solid solution showed the formation of small particles (<3 nm) on the surface (Figure 2d and Supporting Information, Figure S3). EELS characterization revealed that the MgO-supported nanoparticles contain both Fe and Cu. This indicates the presence of a FeO−CuO−MgO solid solution in the raw catalyst. Among the three oxides, CuO is the easiest to reduce because the electronegativity of Cu (1.9) is higher than those of Fe (1.8) or Mg (1.3), resulting in a weaker binding of oxygen[30] to Cu than to either Fe or Mg. The formation of Fe particles indicates that the Fe phase in the solid solution is also reduced at 600 °C, which, lower than the reduction temperature of MgO-supported monometallic Fe catalyst (>700 °C),[24] suggests Cu play an important role in the Fe reduction process. The decrease in Fe ion reduction temperature is attributed to possible spillover of reductive molecules from reduced Cu^{0} in intimate contact with Fe phase in the catalyst.[32−34] Apart from Fe particles distributed over the MgO support, Fe particles anchored on Cu particle (>50 nm) surfaces were also reduced.

When CO is further introduced, SWNTs start to grow on the Fe nanoparticles located not only on MgO (Figure 3a), but also on metallic Cu particles (Figure 3b). Growing carbon nanotubes on the metallic substrate,[35] including Cu with high electrical and thermal conductivities, is important for many applications like displays, cell electrodes, and thermal interface materials.[36] However, in most cases, a diffusion barrier layer[37] between the catalyst and the metal substrate is needed for growing carbon nanotubes. The presence of a barrier layer, however, could increase the contact resistance between carbon nanotubes and the substrate. Our findings here show the possibility of directly growing SWNTs on metallic Cu substrate, which would have potential applications in electrical engineering.[34] Movie S1, Supporting Information, shows the nucleation and growth of an SWNT from MgO-supported Fe nanoparticles. Obviously, the size of the Fe particle determines the diameter of the SWNT. In agreement with previous ETEM studies[38,39] on SWNT growth dynamics, the growth rate of SWNT is inconsistant during the growth process (Figure 3c).

The choice of catalyst support affects the catalyst morphology and the metal−support interactions, thus it has been proved to be crucial for controlled growth of SWNTs.[40,41] Li et al. systematically investigated different kinds of support and concluded that the MgO support is very stable for growing

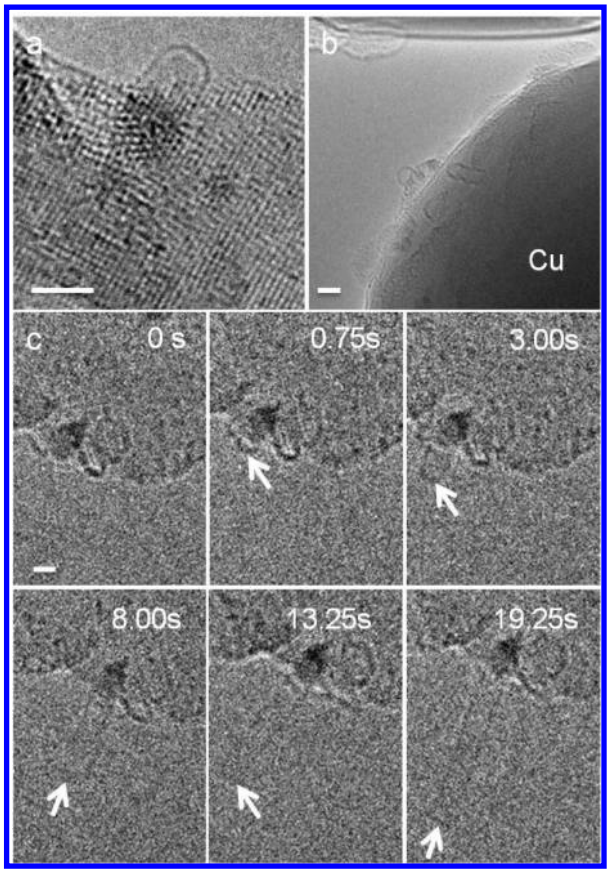

Figure 3. (a) In situ TEM image showing the formation of a SWNT on an MgO-supported Fe particle. (b) In situ TEM image showing the growth of SWNTs on metallic Cu-supported Fe particles. (c) Bright field ETEM image sequence of Fe-catalyzed SWNT growth recorded in 690 Pa CO at 690 °C (extracted from Movie S1, Supporting Information). A time stamp is shown in each image and the arrows indicate the end of the SWNT. Scale bars in all images are 2 nm.

high quality SWNTs.[40] Meanwhile, the MgO support has a strong Lewis basicity,[42] resulting in a strong ability to chemosorb H_2O, which inhibits excessive carbon deposition and prolongs catalyst lifetime. The presence of H_2O on the FeCu/MgO catalyst has been verified in our previous mass spectrometry study.[24] In situ IR was applied to probe the surface chemistry under SWNT growth conditions. Figure 4 shows the time evolution of the IR spectra with the introduction of CO at 600 °C. The absorption bands at 2362 cm^{-1} and 2331 cm^{-1}, characteristics for gas phase CO_2,[43] appeared once when CO was introduced to the catalyst. This indicates the immediate CO oxidation as well as the reduction of CuO and iron oxide. An absorption band corresponding to CO chemisorbed on undercoordinated Mg^{2+} on the surface also arose.[42] Interestingly, a slight increase in the absorption frequency (from 2184 cm^{-1} to 2197 cm^{-1} in 10 min) was observed. The frequency increase results from the effective charge increase of the Mg ions, which is naturally attributed to the structure rearrangement of the catalyst surface after the extraction of Cu^{2+} and Fe^{2+}. This is in agreement with the existence of FeO−CuO−MgO solid solution in the raw catalyst.

On the basis of the in situ ETEM observations and IR investigations on the SWNT growth as well as other ex situ studies, comprehensive mechanisms for carbon nanotube growing on the FeCu/MgO catalyst are proposed, which is

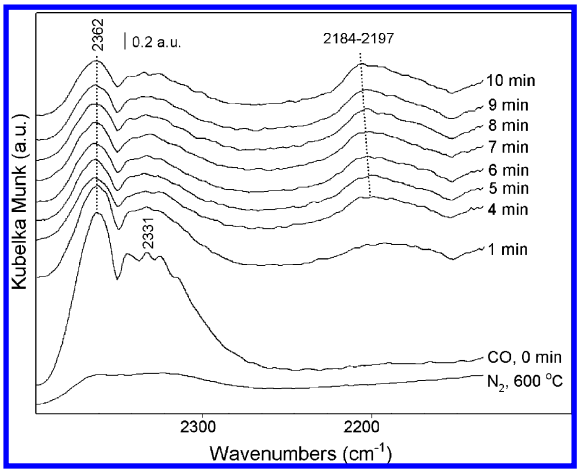

Figure 4. IR spectra of CO absorption on FeCu/MgO catalyst at 600 °C. The recording time is shown above each curve.

schemed in Figure 5. Before introducing CO, Cu is present in the catalyst as CuO particles (>50 nm) and also as a solid

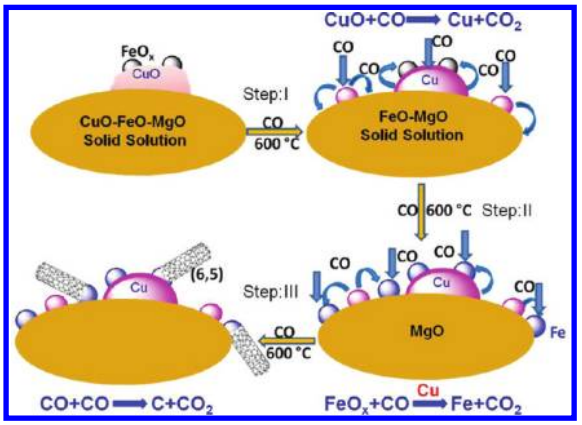

Figure 5. Schematic illustration of SWNT growth on the FeCu/MgO catalyst.

solution with MgO. The CuO phase is reduced to metallic Cu particles in the catalyst after the CO introduction at 600 °C. Small diameter (<3 nm) metallic Cu particles are extracted from the solid solution, and large Cu particles are obtained from reducing CuO particles (>50 nm) originally located on the MgO surface (Step I in Figure 5). The formation of the Cu^0 phase marks the onset of the reduction of the intimate Fe phase to Fe^0 through the proposed spillover of CO species absorbed on Cu^0. As a result, Fe oxide located both in the solid solution and on the large Cu particle surfaces is reduced to metallic Fe nanocrystals stabilized by their supports (Step II in Figure 5). Consequently, growth of SWNTs on the Fe nanocrystals is achieved by prolonged exposure to CO (Step III in Figure 5). On the basis of the understanding of the roles of different components in the catalyst for growing SWNTs, a FeCu catalyst was prepared by the more economic feasible impregnation technique (Supporting Information). The SWNTs grown on the impregnation-prepared FeCu catalyst have a similar chirality distribution as those grown on atomic layer deposition-prepared FeCu catalyst (Supporting Information, Figure S4).

The narrow chirality distribution of the small diameter SWNTs grown at low temperature can be attributed to the

dx.doi.org/10.1021/cm300308k | Chem. Mater. 2012, 24, 1796−1801

limited number of possible caps, which decrease exponentially with decreasing diameter.[44] The cap structure for near-armchair tubes tends to be much more stable than those with relative small chiral angles. Moreover, near armchair SWNTs have relatively lower activation energy for their formation.[29] Therefore, (6,5) and (7,5) tubes are usually the major chiral species in the resulting SWNTs, though their concentrations depend on catalyst compositions and growth parameters.[18,20,45,46] At fixed growth conditions, the catalyst composition plays a dominant role in determining the final chiral distribution of SWNTs.[20,46] As indicated from the relatively low PL intensity ratios between (6,5) to secondary tubes, SWNTs grown from Co and Ni catalysts at ambient pressure usually have relatively large diameter distributions.[45,46] For SWNTs grown on FeCu/MgO catalyst, it is the active Fe catalyst that determines the predominant growth of (6,5) tubes as well as the narrow chirality distribution of the SWNTs.

Besides on the FeCu catalyst, preferential growth of semiconducting SWNTs has also been reported to grow on Co-based catalysts (CoMo[41] and CoMn[23]) despite that high reaction pressure is needed. Considering a common growth parameter shared by the three catalyst systems, it is believed that the low growth temperature accounts for the predominant growth of semiconducting SWNTs. Zoican Loebick et al. attributed such low growth temperature effect to the temperature-related catalyst size and shape.[23] However, the equilibrium shapes of Co and Fe are supposed to be quite different. On the basis of density functional theory, Li et al.[15] investigated the energetic stability of various types of SWNTs. It appears that semiconducting SWNTs exhibited lower formation energies than metallic SWNTs. The calculations suggested that the energies and thermodynamics associated with semiconducting SWNTs are the factors for their preferential growth at low growth temperatures. The hypothesis could also be applicable in the case of low temperature growth of semiconducting SWNTs on the FeCu catalyst.

CONCLUSIONS

SWNTs rich in (6,5) species were successfully grown on MgO-supported FeCu catalyst. The high yield of (6,5) tubes was confirmed by the ED characterization. Furthermore, these nanotubes were shown to be predominantly semiconducting (88%). The preferential growth of SWNTs is attributed to the low growth temperature under which Fe nanoparticles can be reduced with the aid of Cu through a proposed spillover mechanism. ETEM and IR studies suggest the presence of FeO−CuO−MgO solid solution in the catalyst and provide clear evidence of the in situ growth of SWNTs on Fe nanoparticles, which are anchored on either the metallic Cu particles or the MgO support. Such FeCu catalyst is anticipated to be a suitable system for many applications in other CO association/dissociation related catalytic reactions, like Fischer−Tropsch synthesis.

ASSOCIATED CONTENT

Supporting Information

Extensive pictures; preparation of an MgO-supported FeCu catalyst by impregnation; growth and characterization of SWNTs grown on the impregnation prepared FeCu catalyst; an in situ TEM movie showing the growth of a SWNT on a Fe nanoparticle. This material is available free of charge via the Internet at http://pubs.acs.org.

AUTHOR INFORMATION

Corresponding Author

*E-mail: maoshuai.he@aalto.fi (M.H.); esko.kauppinen@aalto.fi (E.I.K.).

Notes

The authors declare no competing financial interest.

ACKNOWLEDGMENTS

This work was supported by the CNB-E Project in Aalto University through the Multidisciplinary Institute of Digitalization and Energy (MIDE) program. The ETEM study was partially funded by the NorTEMnet project. The A. P. Møller and Chastine Mc-Kinney Møller foundation is gratefully acknowledged for the contribution towards the establishment of the Center for Electron Nanoscopy at the Technical University of Denmark.

REFERENCES

(1) Iijima, S.; Ichihashi, T. *Nature* **1993**, *363* (17), 603−605.
(2) Bethune, D. S.; Kiang, C. H.; de Vries, M. S.; Gorman, G.; Savoy, R.; Vazquez, Z.; Beryes, R. *Nature* **1993**, *363*, 605−607.
(3) Iijima, S. *Nature* **1991**, *354*, 56−58.
(4) Dresselhaus, M. S.; Dresselhaus, G.; Saito, R.; Jorio, A. *Phys. Rep.* **2005**, *409* (2), 47−99.
(5) Hersam, M. C. *Nat. Nanotechnol.* **2008**, *3*, 387−394.
(6) Noorden, R. V. *Nature* **2011**, *469*, 14−16.
(7) Wu, Z.; Chen, Z.; Du, X.; Logan, J. M.; Sippel, J.; Nikolou, M.; Kamaras, K.; Reynolds, J. R.; Tanner, D. B.; Hebard, A. F.; et al. *Science* **2004**, *305*, 1273−1276.
(8) Tans, S. J.; Verschueren, A. R. M.; Dekker, C. *Nature* **1998**, *393*, 49−52.
(9) Naumov, A. V.; Kuznetsov, O. A.; Harutyunyan, A. R.; Green, A. A.; Hersam, M. C.; Resasco, D. E.; Nikolaev, P. N.; Weisman, R. B. *Nano Lett.* **2009**, *9* (9), 3203−3208.
(10) Liu, Z.; Zhang, Q.; Qin, L. C. *Phys. Rev. B* **2005**, *71* (24), 245413.
(11) Arnold, M. S.; Green, A. A.; Hulvat, J. F.; Stupp, S. I.; Hersam, M. C. *Nat. Nanotechnol.* **2006**, *1* (1), 60−65.
(12) Nish, A.; Hwang, J.-Y.; Doig, J.; Nicholas, R. J. *Nat. Nanotechnol.* **2007**, *2* (10), 640−646.
(13) Krupke, R.; Hennrich, F.; Lohneysen, H.; Kappes, M. M. *Science* **2003**, *301* (5631), 344−7.
(14) Harutyunyan, A. R.; Chen, G.; Paronyan, T. M.; Pigos, E. M.; Kuznetsov, O. A.; Hewaparakrama, K.; Kim, S. M.; Zakharov, D.; Stach, E. A.; Sumanasekera, G. U. *Science* **2009**, *326* (5949), 116−120.
(15) Li, Y.; Peng, S.; Mann, D.; Cao, J.; Tu, R.; Cho, K. J.; Dai, H. *J. Phys. Chem. B* **2005**, *109* (15), 6968−71.
(16) Hong, G.; Zhang, B.; Peng, B.; Zhang, J.; Choi, W. M.; Choi, J. Y.; Kim, J. M.; Liu, Z. *J. Am. Chem. Soc.* **2009**, *131* (41), 14642−3.
(17) Wang, H.; Wang, B.; Quek, X. Y.; Wei, L.; Zhao, J.; Li, L. J.; Chan-Park, M. B.; Yang, Y.; Chen, Y. *J. Am. Chem. Soc.* **2010**, *132* (47), 16747−9.
(18) Bachilo, S. M.; Balzano, L.; Herrera, J. E.; Pompeo, F.; Resasco, D. E.; Weisman, R. B. *J. Am. Chem. Soc.* **2003**, *125* (37), 11186−11187.
(19) Ding, L.; Tselev, A.; Wang, J.; Yuan, D.; Chu, H.; McNicholas, T. P.; Li, Y.; Liu, J. *Nano Lett.* **2009**, *9* (2), 800−805.
(20) Chiang, W. H.; Mohan Sankaran, R. *Nat. Mater.* **2009**, *8* (11), 882−886.
(21) Zhu, Z.; Jiang, H.; Susi, T.; Nasibulin, A. G.; Kauppinen, E. I. *J. Am. Chem. Soc.* **2011**, *133* (5), 1224−1227.
(22) Jorio, A.; Santos, A.; Ribeiro, H.; Fantini, C.; Souza, M.; Vieira, J.; Furtado, C.; Jiang, J.; Saito, R.; Balzano, L.; et al. *Phys. Rev. B* **2005**, *72* (7), 075207.

(23) Loebick, C. Z.; Podila, R.; Reppert, J.; Chudow, J.; Ren, F.; Haller, G. L.; Rao, A. M.; Pfefferle, L. D. *J. Am. Chem. Soc.* **2010**, *132*, 11125−11131.
(24) He, M.; Chernov, A. I.; Fedotov, P. V.; Obraztsova, E. D.; Sainio, J.; Rikkinen, E.; Jiang, H.; Zhu, Z.; Tian, Y.; Kauppinen, E. I.; et al. *J. Am. Chem. Soc.* **2010**, *132* (40), 13994−6.
(25) Zuo, J. M.; Vartanyants, I.; Gao, M.; Zhang, R.; Nagahara, L. A. *Science* **2003**, *300* (5624), 1419−21.
(26) Qin, L. C.; Ichihashi, T.; Iijima, S. *Ultramicroscopy* **1997**, *67*, 181−189.
(27) Jiang, H.; Nasibulin, A.; Brown, D.; Kauppinen, E. *Carbon* **2007**, *45* (3), 662−667.
(28) Ding, F.; Harutyunyan, A. R.; Yakobson, B. I. *Proc. Natl. Acad. Sci.* **2009**, *106* (8), 2506−2509.
(29) Wang, Q.; Ng, M. F.; Yang, S. W.; Yang, Y.; Chen, Y. *ACS Nano* **2010**, *4* (2), 939−46.
(30) Hu, Y. H.; Ruckenstein, E. *Catal. Rev.* **2002**, *44* (3), 423−453.
(31) Cordischi, D.; Pepe, F.; Schiaveelo, M. *J. Phys. Chem.* **1973**, *77*, 1240−1245.
(32) Wielers, A. H. F.; Koebrugge, G. W.; Geus, J. W. *J. Catal.* **1990**, *121*, 375−385.
(33) de Smit, E.; de Groot, F. M.; Blume, R.; Havecker, M.; Knop-Gericke, A.; Weckhuysen, B. M. *Phys. Chem. Chem. Phys.* **2010**, *12* (3), 667−80.
(34) Wachs, I. E.; Dwyer, D. J.; Iglesia, E. *Appl. Catal.* **1984**, *12*, 201−207.
(35) Talapatra, S.; Kar, S.; Pal, S. K.; Vajtai, R.; Ci, L.; Victor, P.; Shaijumon, M. M.; Kaur, S.; Nalamasu, O.; Ajayan, P. M. *Nat. Nanotechnol.* **2006**, *1* (2), 112−116.
(36) Wang, H.; Feng, J. Y.; Hu, X. J.; Ng, K. M. *J. Phys. Chem. C* **2007**, *111* (34), 12617−12624.
(37) Lin, W.; Zhang, R. W.; Moon, K. S.; Wong, C. P. *IEEE Trans. Adv. Packag.* **2010**, *33* (2), 370−376.
(38) Hofmann, S.; Sharma, R.; Ducati, C.; Du, G.; Mattevi, C.; Cepek, C.; Cantoro, M.; Pisana, S.; Parvez, A.; Cervantes-Sodi, F.; et al. *Nano Lett.* **2007**, *7* (3), 602−608.
(39) Yoshida, H.; Takeda, S.; Uchiyama, T.; Kohno, H.; Homma, Y. *Nano Lett.* **2008**, *8* (7), 2082−6.
(40) Li, Q. W.; Yan, H.; Cheng, Y.; Zhang, J.; Liu, Z. F. *J. Mater. Chem.* **2002**, *12* (4), 1179−1183.
(41) Lolli, G.; Zhang, L.; Balzano, L.; Sakulchaicharoen, N.; Tan, Y.; Resasco, D. E. *J. Phys. Chem. B* **2006**, *110* (5), 2108−2115.
(42) Davydov, A. *Molecular Spectroscopy of Oxide Catalyst Surfaces*; John Wiley & Sons Ltd: New York, 2003.
(43) Wasylenko, W.; Frei, H. *Phys. Chem. Chem. Phys.* **2007**, *9* (40), 5497−502.
(44) Astakhova, T. Y.; Buzulukova, N. Y.; Vinogradov, G. A.; Osawa, E. *Fullerene Sci. Technol.* **1999**, *7* (2), 223−237.
(45) He, M.; Chernov, A. I.; Fedotov, P. V.; Obraztsova, E. D.; Rikkinen, E.; Zhu, Z.; Sainio, J.; Jiang, H.; Nasibulin, A. G.; Kauppinen, E. I.; et al. *Chem. Commun.* **2011**, *47* (4), 1219−21.
(46) He, M.; Chernov, A. I.; Obraztsova, E. D.; Sainio, J.; Rikkinen, E.; Jiang, H.; Zhu, Z.; Kaskela, A.; Nasibulin, A. G.; Kauppinen, E. I.; et al. *Nano Res.* **2011**, *4* (4), 334−342.